

Analysis and Implementation of Analog 4f Optical System and Digital Spatial Filtering Techniques for Image Processing

JUAN SEBASTIAN AGUIAR-CASTRILLON^{1,*} AND RAUL ANDRES CASTAÑEDA-QUINTERO¹

¹School of Applied Sciences and Engineering, EAFIT University, Carrera 49 N 7 Sur 50, Medellin, Antioquia, 050022, Colombia.

*jsaguiarc@eafit.edu.co

Compiled October 23, 2024

This report investigates spatial filtering techniques using both an analog 4f system with fabric and digital methods applied to various images, including Lenna (with Gaussian noise), a newspaper drawing, the Colombian 20 pesos bill, "Xilography by Jost Amman," and a map of Colombia with regional patterns. Low-pass filters smoothed the images, while high-pass filters enhanced edges and fine details. In the 4f system, image inversion was confirmed. Additionally, reducing the pinhole size or increasing the obstacle size increased the Mean Squared Error (MSE) and decreased Pearson Correlation Coefficient (PCC), while high-pass filtering caused grayscale inversion. Digital filtering offered greater flexibility, allowing easier manipulation of the Fourier plane and mask applications. Gaussian noise in the Lenna image was reduced to an MSE of 16 and a PCC of 0.82. Low-pass filters removed print marks from the newspaper drawing. Using masks eliminated text from the 20 pesos bill without distorting other features. Filtering the xylograph ranged from smoothing to sharpening fine details, and a band-pass filter with a 30-pixel ring mask filtered patterns in the Colombian map by adjusting its position in the Fourier plane.

Repository: <https://github.com/Aguiario/Analogic-and-Digital-Spatial-Filtering.git>

1. INTRODUCTION

A 4f optical system is an essential configuration in optical image processing, consisting of two lenses spaced by the sum of their focal lengths to perform a Fourier transform and its inverse [1]. This arrangement grants direct access to an image's spatial frequency components, enabling frequency-domain filtering. By placing spatial filters at the Fourier plane, specific frequencies can be blocked or passed, allowing for applications like edge enhancement, noise reduction, and feature extraction [1]. Widely used in microscopy, holography, and optical computing [2], this report compares analog spatial filtering using a 4f system with digital techniques, exploring their advantages and applications. It covers image formation, frequency spectrum analysis, and filtering with various low-pass and high-pass filters, providing a comparison of analog versus digital methods.

2. THEORETICAL BACKGROUND

A. Fourier Transforms

The Fourier transform is a mathematical tool that decomposes a spatial signal, such as an image, into its frequency components. In optical systems, the Fourier transform is useful because it describes how light can be manipulated in the spatial frequency domain, allowing for spatial filtering and image processing[3].

When a transmittance $g(x, y)$ is shifted in the spatial domain by (x_0, y_0) , its Fourier transform is modified by a phase factor. The shifted transmittance can be represented as $g(x - x_0, y - y_0)$ [3]. The Fourier transform of this shifted function is:

$$\mathcal{F}\{g(x - x_0, y - y_0)\} = G(f_x, f_y)e^{-2\pi i(f_x x_0 + f_y y_0)} \quad [3]. \quad (1)$$

This result demonstrates that shifting the input transmittance in the spatial domain leads to phase modulation in the frequency domain, while leaving the amplitude unchanged.

A.1. Fraunhofer Transform in 4f Systems

The Fraunhofer transform, or far-field approximation, describes the diffraction pattern when light passes through an aperture and the observation plane is distant. The resulting pattern is the Fourier transform of the aperture's transmittance function $g(x, y)$, with the complex amplitude $U(f_x, f_y)$ at the observation plane. The complex amplitude $U(f_x, f_y)$ at the observation plane is given by:

$$U(f_x, f_y) \propto \frac{1}{\lambda z} \mathcal{F}\{g(x, y)\} \quad [3], \quad (2)$$

where λ is the wavelength of light, z is the distance from the aperture to the observation plane, and $\mathcal{F}\{g(x, y)\}$ represents the Fourier transform of the aperture function[3].

Lenses perform a Fraunhofer transform by projecting the far-field diffraction pattern onto a finite plane known as the Fourier plane, facilitating spatial frequency manipulation. They introduce a phase shift to incoming wavefronts, causing predictable convergence or divergence. When a parallel, collimated light beam passes through a lens, the rays bend based on the angle of incidence, converging at the focal point. This convergence maps spatial positions in the object plane to spatial frequencies in the focal plane [3]. Specifically, when $z = f$ (the focal length), the spatial frequencies of the incoming light are accurately mapped to the observation plane.

The 4f system is a classic optical setup that utilizes two lenses, each positioned at a distance equal to their focal lengths from the object and from each other, to perform sequential Fourier and inverse Fourier transforms[1].

The first lens, situated one focal length from the object (e.g., a transparency with the transmittance function $g(x, y)$), conducts a Fourier transform, converting spatial information into the frequency domain. The mathematical representation of this process is given by the equation:

$$U_1(f_x, f_y) = \frac{1}{\lambda f} \mathcal{F}\{g(x, y)\} H(f_x, f_y) [3], \quad (3)$$

where $U_1(f_x, f_y)$ denotes the resulting field in the Fourier plane.

Within this Fourier plane, spatial filters can be applied, represented by a transfer function $H(f_x, f_y)$. These filters selectively block or transmit specific frequency components. For instance, a low-pass filter is designed to remove high-frequency components that correspond to fine details, while a high-pass filter eliminates low-frequency components associated with smooth variations[4].

After filtering, the second lens, placed one focal length away from the Fourier plane, performs an inverse Fourier transform. This converts the frequency-domain data back into spatial information, reconstructing the filtered image in the image plane. The resulting output image is:

$$U_2(x', y') = \mathcal{F}^{-1}\{U_1(f_x, f_y)\} = g(-x', -y') [5]. \quad (4)$$

This inverse Fourier transform flips the image both horizontally and vertically. The inversion occurs because each lens in the system introduces a sign change in the spatial coordinates due to the nature of the Fourier transform. Specifically, the Fourier transform converts spatial positions into frequency components, and when the inverse transform is applied, it restores the original positions but with reversed signs in both axes. This results in an inverted image[6].

B. Spatial Filtering

Spatial filtering modifies an image's frequency content by manipulating its Fourier components in the frequency plane. In a 4f system, filters are applied at the Fourier plane between two lenses [3]. The main types are low-pass and high-pass filters.

B.1. Low-pass and High-pass Filters

Low-pass filters allow low spatial frequencies to pass while attenuating higher ones, smoothing the image and removing fine details and noise. The cutoff frequency f_c specifies the highest frequency permitted:

$$H(f_x, f_y) = \begin{cases} 1, & \sqrt{f_x^2 + f_y^2} \leq f_c, \\ 0, & \text{otherwise.} \end{cases} [7] \quad (5)$$

High-pass filters, on the other hand, block low frequencies and enhance high frequencies, improving edges and fine details:

$$H(f_x, f_y) = \begin{cases} 0, & \sqrt{f_x^2 + f_y^2} \leq f_c, \\ 1, & \text{otherwise.} \end{cases} [7] \quad (6)$$

By selectively blocking or allowing certain frequencies, these filters control the sharpness, contrast, and overall appearance of the image, band-pass filters are understood as a combination of low and high pass filters.

3. METHODOLOGY

A. 4f Optical System Setup

The 4f optical system was set up for spatial filtering using low-pass and high-pass filters, as illustrated in Fig. 1. It begins with a red He-Ne laser (633 nm, 156 mW)[8], which provides a coherent light source. The laser beam passes through a neutral density filter to control intensity and protect the camera from overexposure, followed by a beam expander to collimate and increase diameter. The beam then reaches a transparency holder containing various objects for image processing. The first lens, positioned about 15 cm from the transparency, performs a Fourier transform on the light, mapping spatial information into the frequency domain. At the Fourier plane, a spatial filter (low-pass or high-pass) is introduced. The second lens, also 15 cm away, performs an inverse Fourier transform, converting the filtered frequency information back to the spatial domain. Finally, the processed image is captured by a digital camera (DMK 23U445[9]) positioned at the image plane, allowing for saving, analysis and comparison of the filtering methods used.

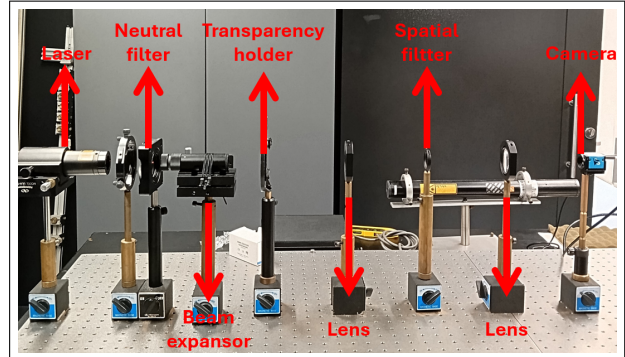


Fig. 1. The 4f optical system setup, showing the positions of each element.

B. Part I: Image Inversion

This experiment aimed to confirm the image inversion produced by the 4f optical system using the transparency shown in Fig. 2, placed at the object plane.



Fig. 2. Transparency sample used to verify the inversion.

C. Part II: Experimental Spatial Filtering

This section focuses on applying spatial filters in the 4f optical system. Both low-pass and high-pass filters will use to manipulate the frequency content of the image and observe the resulting effects on image sharpness, contrast, and resolution.

C.1. Low-pass Filter

A low-pass filter is implemented by varying the aperture of a diaphragm iris, simulating a pinhole with different sizes. The higher spatial frequencies that pass through the system will limit by adjusting the aperture, allowing for the analysis of how the fabric's structure influences the resulting image in terms of spatial frequency, resolution, and contrast. A fabric with periodic structure are placed in the transparency holder, acting as diffraction gratings and generating diffraction patterns with distinct spatial frequency components, as shown in Fig. 3. The periodic openings and symmetries of the fabric produce diffraction orders, which appear as concentrated spots in the frequency spectrum.

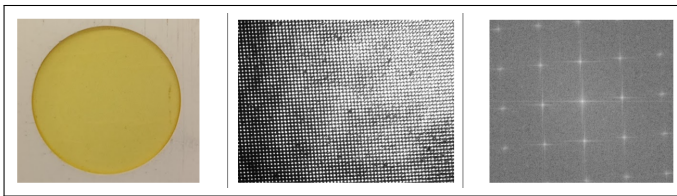


Fig. 3. Fabric sample used in the spatial filtering low-pass experiment. Left: the fabric sample; center: its diffraction pattern after passing through the 4f system without a filter; right: its Fourier transform.

Next, the transparent object shown in Fig. 4, which depicts Emperor Maximilian, served as the input image for the low-pass and high-pass filtering experiments. In Fig. 4, two squares—one red and one yellow—highlight the regions of interest where the beam will be focused. The filtering will also be performed by modulating the diaphragm iris.



Fig. 4. Transparency used in low-pass and high-pass spatial filtering experiments. The red square highlights the dress, and the yellow square highlights the hair.

C.2. High-pass Filter

To perform high-pass filtering, opaque obstacles in the form of circles and slits with varying widths were positioned at the Fourier plane to block low frequencies in the previously mentioned transparency (see Fig. 4). The circular obstacles obstructed the lower spatial frequencies near the optical axis, allowing only the higher frequencies to pass through. Additionally, slits of various widths were enable the selective passage of horizontal or vertical frequencies, depending on their orientation. Fig. 5 illustrates the circular obstacles with diameters of 0.25 mm, 0.5 mm, and 1 mm, as well as the slits measuring 0.25 mm, 0.5 mm, 1 mm, and 1.25 mm.

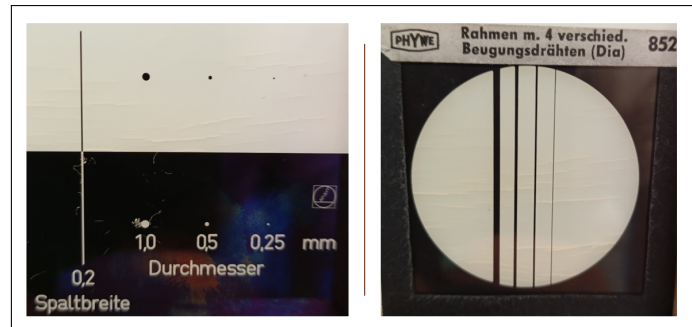


Fig. 5. High-pass filtering setup: circular obstacles (left) and slits (right) with varying widths.

D. Part III: Computational Spatial Filtering

Spatial filtering was applied to digital images using Python to compute their Fourier transforms and analyze the effects of filters. The fundamental algorithm, illustrated in Fig. 6 and the complete code is available in the open-source lab repository.

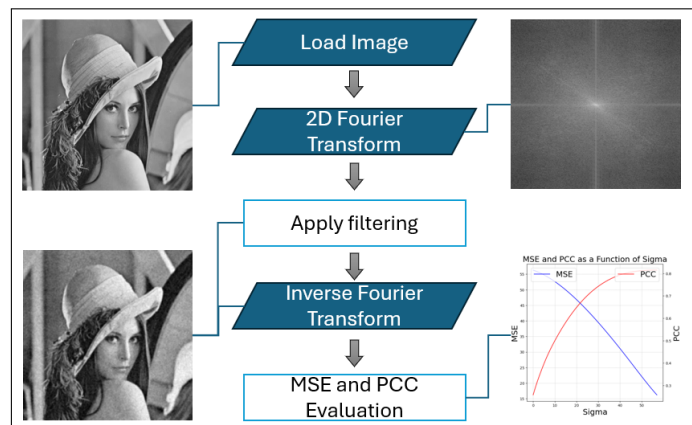


Fig. 6. Basic algorithm for spatial frequency processing using Fourier transforms.

The digital image processing experiments utilizing the images shown in Fig. 7 are explained below:

- **Lenna Image Processing:** This experiment applied a digital filter to the Lenna image, which contains Gaussian noise (panel a), to evaluate noise reduction by comparing the filtered image with the original.
- **Newspaper Print Analysis:** The print patterns of a newspaper drawing (panel b) was analyzed for the regularity of

black dot patterns against a white background, aiming to remove filling effects while preserving image contours.

- **20-Peso Bill Examination:** The Colombian 20-peso bill (panel c) was analyzed spatial frequency characteristics of the fine text like the word “CALDAS” and remove it using digital filtering.
- **Xilography Analysis:** The xilography by Jost Amman (panel d) was examined for its complex patterns, exploring digital filters to enhance or isolate specific elements within the artwork.

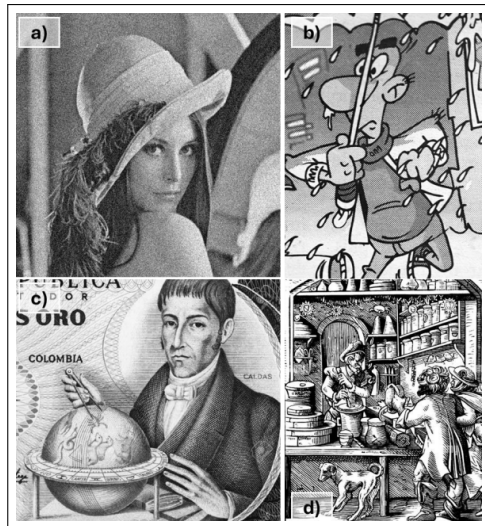


Fig. 7. Images utilized in the image processing experiments: a) Lenna image, b) newspaper print, c) Colombian 20-peso bill, d) xilography by Jost Amman.

- **Colombian Map Filtering:** A digital map of Colombia was created (see Fig. 8), where each department is represented by a unique spatial frequency pattern and pattern is shared among departments within the same region. The objective is to apply digital filters to selectively extract information from specific regions and isolate spatial frequency components for filtering.

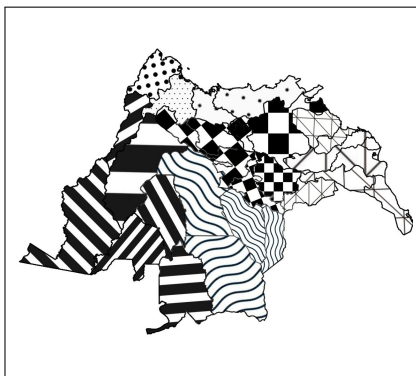


Fig. 8. Colombian map with spatial frequency patterns for regional filtering.

E. Analysis tools used

In the context of image processing, especially when comparing the Fourier spectra of an original and filtered image, two common metrics used for comparison are the **Mean Squared Error (MSE)** and the **Pearson Correlation Coefficient**. These metrics provide insight into the similarity between two images' frequency components, helping us understand how much a filtering process has altered the image in the frequency domain.

E.1. Mean Squared Error (MSE)

MSE is a statistical measure that quantifies the average of the squared differences between corresponding values in two datasets. In this context, it compares the magnitude spectra of the original and filtered images in the frequency domain, defined mathematically as:

$$\text{MSE} = \frac{1}{N} \sum_{i=1}^N (X_i - Y_i)^2 [10], \quad (7)$$

where X_i and Y_i are the magnitude values of the Fourier-transformed original and filtered images, respectively, and N is the total number of pixels. A lower MSE value indicates greater similarity between the filtered and original images' frequency content, while a higher MSE suggests significant differences [10].

E.2. Pearson Correlation Coefficient (PCC)

PCC measures the linear correlation between two variables, indicating how closely changes in one variable relate to changes in another. For comparing the Fourier magnitude spectra of two images, the formula is:

$$r = -\frac{\sum_{i=1}^N (X_i - \bar{X})(Y_i - \bar{Y})}{\sqrt{\sum_{i=1}^N (X_i - \bar{X})^2 \sum_{i=1}^N (Y_i - \bar{Y})^2}} [11], \quad (8)$$

where X_i and Y_i are the magnitude values of the original and filtered Fourier-transformed images, and \bar{X} and \bar{Y} are their mean values. The correlation coefficient r ranges from -1 to 1 . A higher r value indicates that the filtering process has preserved the overall structure of the image, while a lower r suggests significant differences in frequency components, indicating the introduction or suppression of frequencies[11].

4. RESULTS

A. Image Inversion Analysis

The captured image of the car, shown in Fig. 9, was inverted both horizontally and vertically after passing through the system.

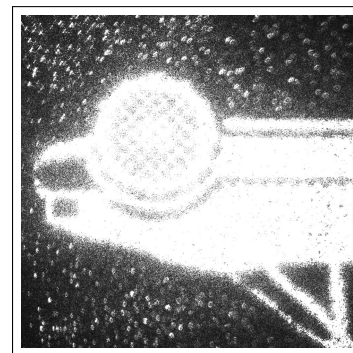


Fig. 9. Inverted image of a car after passing through the 4f optical system.

B. Low-Pass Filter Effects

Fig. 10 shows the results from the experiment using fabric. The findings indicate that the 1.5 mm aperture achieved MSE of 1.4970 and a PCC of 0.3667, while the 1.0 mm aperture resulted in an MSE of 2.7869 and a PCC of 0.3275.

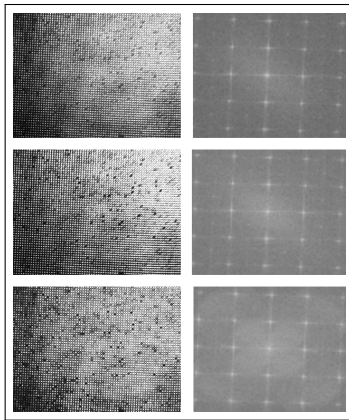


Fig. 10. Results of the low-pass filtering experiment using fabric: (Top) unfiltered image, (Middle) filtered with a 1.5 mm pinhole, (Bottom) filtered with a 1 mm pinhole.

Fig. 11 shows the results of applying low-pass filters to two regions of Maximiliano's transparency from **Fig. 4**. The first row displays the unfiltered image, the second row shows the image filtered with a 1.5 mm pinhole, and the last row presents the 1.0 mm pinhole filter.

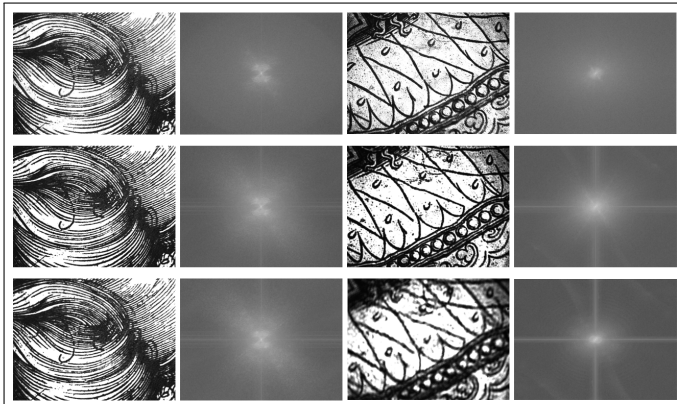


Fig. 11. Results of the low-pass filtering experiment applied to transparency.

Table 1 summarizes the MSE and PCC data obtained from the low-pass experiments.

Table 1. MSE and PCC for Low-Pass Filtering Experiments

Experiment	MSE	PCC
Hair (1.5 mm pinhole)	2.1132	0.5628
Dress (1.5 mm pinhole)	5.0267	0.5290
Hair (1.0 mm pinhole)	2.8088	0.5430
Dress (1.0 mm pinhole)	6.3692	0.4486

C. High-Pass Filter Effects

Similar to **Fig. 11**, **Fig. 12** shows the results of applying high-pass filters to the same regions. The first row presents the image filtered with a circular obstacle of 0.25 mm diameter, the second row with a 0.5 mm diameter one, and the last row depicts with a 1.0 mm diameter one.

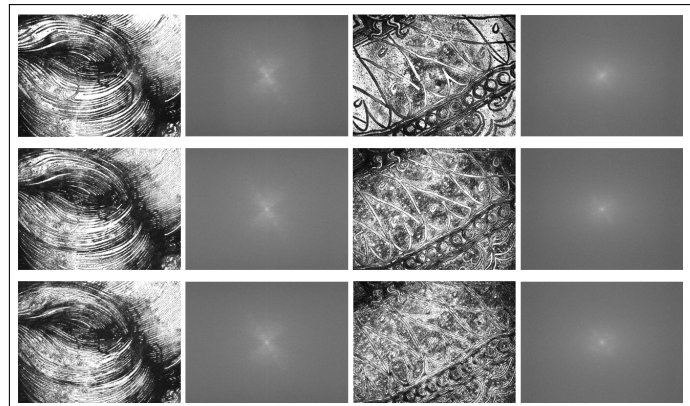


Fig. 12. Results of the high-pass filtering experiment applied to transparency.

Table 1 summarizes the Mean Squared Error (MSE) and Peak Correlation Coefficient (PCC) data obtained from the high-pass experiments.

Table 2. MSE and PCC for High-Pass Filtering Experiments

Experiment	MSE	PCC
Hair (0.25 mm diameter)	0.8277	0.4651
Dress (0.25 mm diameter)	0.8879	0.4167
Hair (0.5 mm diameter)	0.8924	0.4137
Dress (0.5 mm diameter)	0.9954	0.3902
Hair (1.0 mm diameter)	0.9101	0.4051
Dress (1.0 mm diameter)	1.0721	0.3764

A similar effect occurs when using a slit as the obstacle. However, the filtering becomes concentrated in specific areas of the image, projecting the slit's shape onto the filtered result as shown in **Fig. 13**.

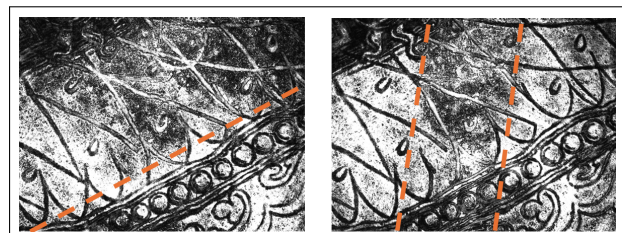


Fig. 13. High-pass filtering experiment using a 0.25 mm slit applied to the transparency. Left: placed horizontally. Right: placed vertically.

D. Lenna Image Processing

The results of filtering an image with Gaussian noise are shown in Fig. 14. By adjusting the sigma parameter of a low-pass filter, the goal was to minimize the mean squared error (MSE) and maximize the Pearson correlation coefficient (PCC). The results indicate that with a sigma value of 62 pixels, achieving an MSE of approximately 16.22 and a PCC of 0.82.

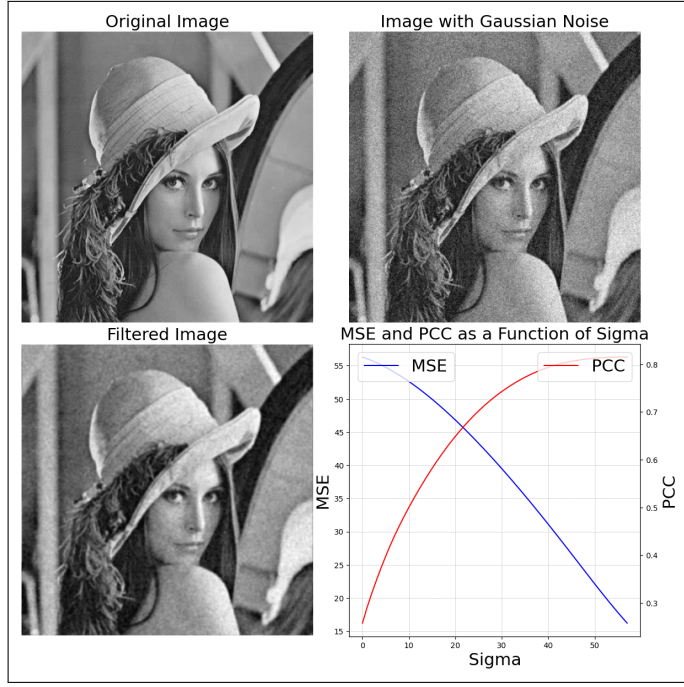


Fig. 14. Results: top left - original image, top right - noisy image, bottom left - filtered image, bottom right - variation of sigma.

E. Newspaper Print Analysis

In this experiment, the limit sigma was calculated, which is the point at which no low-pass filtering occurs; specifically, when MSE equals 0 and PCC equals 1. It was determined that this value is 230. Using this result, filters of one-sixth and one-eighth of this sigma were applied, the results is shown in Fig. 15.

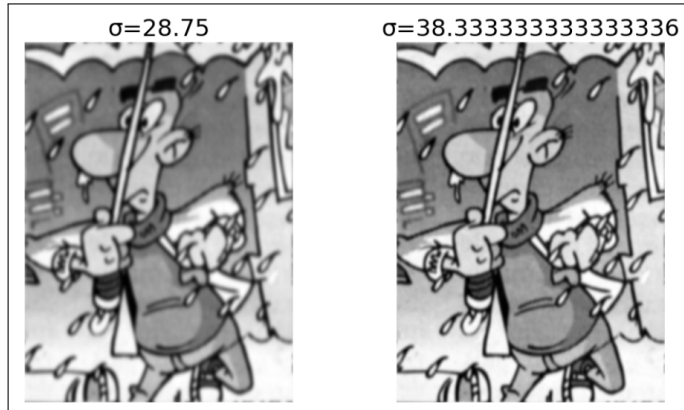


Fig. 15. Results of applying filters set to sigma = 28.75 & 38.3

F. 20-Peso Bill Analysis

Fig. 16 shows the result of isolating the frequencies corresponding to the words "Colombia" and "Caldas" by creating a mask and filtering them from the original image from Fig. 7.

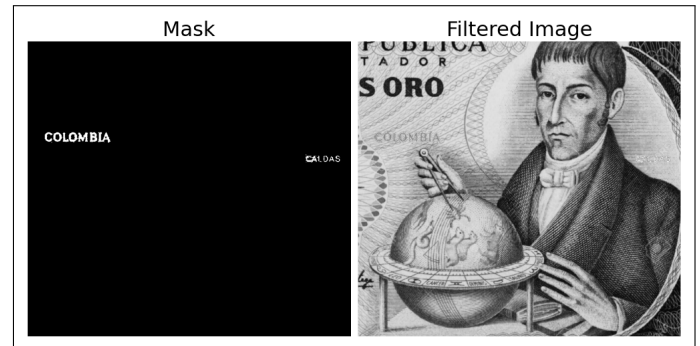


Fig. 16. Result of applying a selective filter to isolate the words "Colombia" and "Caldas".

G. Xilography Analysis

The experiment in Fig. 17 presents the results after applying three filters: the first filter smooths the image by averaging pixel values with their neighbors; the second filter reduces noise through Gaussian-weighted blurring; and the third filter enhances edges and fine details by emphasizing contrasts between pixels.

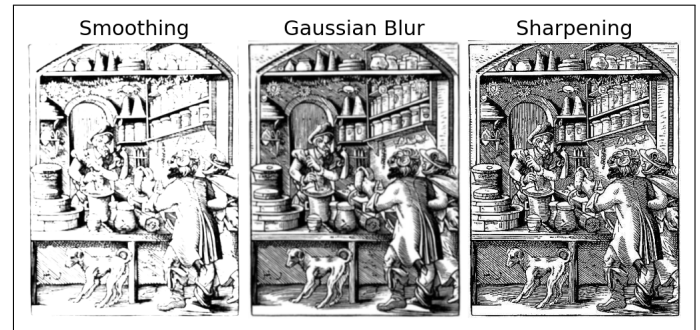


Fig. 17. Results of applying three different image filters.

H. Colombian Map Filtering

The results shown in Fig. 18 illustrate the application of a ring mask to create a bandpass filter with cutoff frequencies of 20 and 50 pixels, resulting in a filter bandwidth of 30 pixels. Various placements of the mask within the Fourier spectrum were employed for filtering, with the coordinates (0, 0) defined as the center of the image.

5. DISCUSSION

The results demonstrate significant findings across various experiments. Initially, Fig. 9 confirms the theoretical predictions regarding image inversion, as discussed in Eq. 4, corroborated by Katkovnik et al. [5].

In the analog spatial filtering using the 4f system, Fig. 10 shows that reducing the iris diaphragm aperture leads to a concentrated Fourier spectrum indicative of the fabric's diffraction

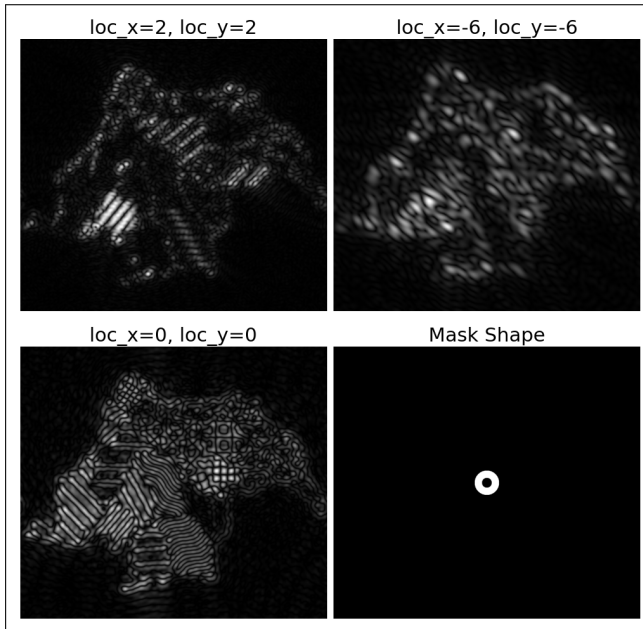


Fig. 18. Filtering using a ring 30-pixels bandpass mask.

pattern. For a 1 mm aperture, PCC is 0.32, while MSE rises by approximately 2.8, illustrating the blurring effects of low-pass filtering and the loss of fine details. A similar trend is observed in Maximiliano's image, detailed in Fig. 11, where a smaller aperture increases blurriness and concentrates intensity maxima in the Fourier plane, indicating the removal of high frequencies. The quantitative analysis in Table 1 reveals a significant drop in PCC and a sixfold increase in MSE for the 1 mm aperture.

High-pass filtering also exhibits increased MSE and decreased PCC but enhancing small details, resulting in a near-inverted grayscale image. This highlights how high-pass filtering amplifies high-frequency components responsible for fine details, enhancing contrast and visibility. The effects of slit size on filtering quality were also noted; when the slit size aligns with the analysis area, it projects solely onto that region, leading to asymmetric filtering responses. In contrast, a circular obstacle would yield more uniform results, emphasizing the influence of shape and size on frequency distribution.

Transitioning to digital processing, Gaussian noise in the Lena image was effectively reduced using a 62-pixel low-pass filter, lowering MSE from over 55 to 16.22 and increasing PCC from 0 to 0.82. Despite potential MSE increases due to image smoothing, this experiment showed a remarkable preservation of relevant details, validating the effectiveness of the filtering technique. Similar results were observed with print marks in a drawing, where low-pass filters of 28.75 and 38.3 pixels reduced noise while maintaining contour integrity, which is vital for applications requiring shape accuracy. These findings underscore the relationship between high frequencies and fine details in images, confirming that low-pass filters can effectively smooth images while preserving structural features.

The versatility and efficacy of digital processing were further illustrated in experiments involving the 20-peso bill, xylophonist analysis, and pattern filtering in the map of Colombia. In the first experiment, the filtering of the words "COLOMBIA" and "CALDAS" effectively removed them, with "CALDAS" demonstrating near-complete elimination, as shown in Fig. 16. The

xylophonist experiment highlighted the creative potential of various filters, presented in Fig. 17. A low-pass filter smoothed the image by removing small details, while a Gaussian blur further diffused it, retaining general characteristics but reducing sharpness. A sharpening filter, acting as a high-pass filter, enhanced lines and contours, crucial for detailed analysis. Finally, the map of Colombia employed Fourier domain filtering, concentrating filter masks to visualize specific patterns. Fig. 18 illustrates how the department of Vaupés was isolated at location (2,2), revealing dominant patterns, while location (0,0) exhibited the prevalence of line patterns, showcasing the capability of digital processing to uncover hidden structures and patterns in spatial data.

6. CONCLUSION

The experiments demonstrated the principles of image inversion and spatial filtering, confirming the significant impact of aperture size on image clarity. Low-pass filtering techniques proved effective in reducing Gaussian noise while preserving essential details, highlighting their utility in enhancing image quality for further analysis. In contrast, high-pass filters successfully accentuated fine details, underscoring the importance of high-frequency components in visual interpretation. Additionally, the versatility of digital processing was showcased through its ability to isolate specific features in complex images, which is vital for applications in pattern recognition and spatial data analysis. Overall, these findings emphasize the need for careful selection of filtering techniques to achieve a balance between detail preservation and noise reduction.

REFERENCES

1. K. Fedus and G. Boudebs, "Experimental techniques using 4f coherent imaging system for measuring nonlinear refraction," *Opt. Commun.* **292**, 140–148 (2013).
2. L. Yaroslavsky, "Optical transforms in digital holography," in *Holography 2005: International Conference on Holography, Optical Recording, and Processing of Information*, vol. 6252 Y. Denisyuk, V. Sainov, and E. Stoykova, eds., International Society for Optics and Photonics (SPIE, 2006), p. 625216.
3. O. K. Ersoy, *Diffraction, Fourier Optics and Imaging* (John Wiley & Sons, Inc., 2006).
4. M. Roth, J. Heber, and K. Janschek, "System design of programmable 4f phase modulation techniques for rapid intensity shaping: a conceptual comparison," in *Laser-based Micro- and Nanoprocessing X*, vol. 9736 U. Klotzbach, K. Washio, and C. B. Arnold, eds., International Society for Optics and Photonics (SPIE, 2016), p. 97361G.
5. V. Katkovnik and J. Astola, "Phase retrieval via spatial light modulator phase modulation in 4f optical setup: numerical inverse imaging with sparse regularization for phase and amplitude," *J. Opt. Soc. Am. A* **29**, 105–116 (2012).
6. C. Gao, D. Wang, K. Qiao *et al.*, "Optical system design of fully symmetrical fourier transform lens," *Opt. Rev.* **28**, 349–357 (2021).
7. A. Makandar and B. Halalli, "Image enhancement techniques using highpass and lowpass filters," *Int. J. Comput. Appl.* **109**, 12–15 (2015).
8. "Red helium-neon (hene) lasers," <https://www.newport.com/c/helium-neon-lasers> (2024). Accessed: 2024-10-18.
9. "Dmk 23u445 monochrome camera," <https://www.1vision.co.il/products/archive/dmk-23u445> (2017). Accessed: 2024-10-18.
10. C. C. B. Jr. and C. L. Matson, "Using mean-squared error to assess visual image quality," in *Advanced Signal Processing Algorithms, Architectures, and Implementations XVI*, vol. 6313 F. T. Luk, ed., International Society for Optics and Photonics (SPIE, 2006), p. 63130E.
11. J. Benesty, J. Chen, and Y. Huang, "On the importance of the pearson correlation coefficient in noise reduction," *IEEE Trans. on Audio, Speech, Lang. Process.* **16**, 757–765 (2008).